



Published in final edited form as:

*Cancer Gene Ther.* 2012 September ; 19(9): 630–636. doi:10.1038/cgt.2012.41.

## Intravenous Administration of Adenoviruses Targeting Transforming Growth Factor Beta Signaling Inhibits Established Bone Metastases in 4T1 Mouse Mammary Tumor Model in an Immunocompetent Syngeneic Host

Zhenwei Zhang<sup>1,\*</sup>, Zebin Hu<sup>1,\*</sup>, Janhavi Gupta<sup>1</sup>, Jeffrey Krimmel<sup>1</sup>, Helen Gerseny<sup>1</sup>, Arthur Berg<sup>1</sup>, John Robbins<sup>1</sup>, Hongyan Du<sup>2</sup>, Bellur Prabhakar<sup>3</sup>, and Prem Seth<sup>1,#</sup>

<sup>1</sup>Gene Therapy Program, Department of Medicine, NorthShore Research Institute, Evanston, IL

<sup>2</sup>Center for Clinical and Research Informatics, NorthShore Research Institute, Evanston, IL, an Affiliate of the University of Chicago, Chicago, IL

<sup>3</sup>Department of Microbiology and Immunology, the University of Illinois at Chicago, Chicago, IL

### Abstract

We have examined the effect of adenoviruses expressing soluble transforming growth factor receptorII-Fc (sTGFβRIIFc) in a 4T1 mouse mammary tumor bone metastasis model using syngeneic BALB/c mice. Infection of 4T1 cells with a non-replicating adenovirus, Ad(E1-).sTβRFc, or with two oncolytic adenoviruses, Ad.sTβRFc and TAd.sTβRFc, expressing sTGFβRIIFc (the human TERT promoter drives viral replication in TAd.sTβRFc) produced sTGFβRIIFc protein. Oncolytic adenoviruses produced viral replication and induced cytotoxicity in 4T1 cells. 4T1 cells were resistant to the cytotoxic effects of TGFβ-1 (up to 10 ng/ml). However, TGFβ-1 induced the phosphorylation of SMAD2 and SMAD3, which were inhibited by co-incubation with sTGFβRIIFc protein. TGFβ-1 also induced IL-11, a well-known osteolytic factor. Intracardiac injection of 4T1-luc2 cells produced bone metastases by day 4. Intravenous injection of Ad.sTβRFc (on days 5 and 7) followed by bioluminescence imaging (BLI) of mice on days 7, 11 and 14 in tumor bearing mice indicated inhibition of bone metastasis progression (p<0.05). X-ray radiography of mice on day 14 showed a significant reduction of the lesion size by Ad.sTβRFc (p<0.01) and TAd.sTβRFc (p<0.05). Replication-deficient virus Ad(E1-).sTβRFc expressing sTGFβRIIFc showed some inhibition of bone metastasis, while Ad(E1-).Null was not effective in inhibiting bone metastases. Thus, systemic administration of Ad.sTβRFc and TAd.sTβRFc can inhibit bone metastasis in the 4T1 mouse mammary tumor model, and can be developed as potential anti-tumor agents for breast cancer.

Users may view, print, copy, download and text and data- mine the content in such documents, for the purposes of academic research, subject always to the full Conditions of use: [http://www.nature.com/authors/editorial\\_policies/license.html#terms](http://www.nature.com/authors/editorial_policies/license.html#terms)

<sup>#</sup>Corresponding Author. Prem Seth, PhD, Gene Therapy Program, Department of Medicine, NorthShore Research Institute, an affiliate of the University of Chicago, Evanston Hospital, 2650 Ridge Ave, Room B 652, Evanston, IL 60201. [pseth@northshore.org](mailto:pseth@northshore.org).

<sup>\*</sup>These co-authors made equal contribution

Present address: Department of Experimental Hematology, Beijing Institute of Radiation Medicine, Beijing, China

## Keywords

Breast cancer; mouse model; TGF $\beta$ ; oncolytic adenovirus; systemic delivery

---

## Introduction

In the United States alone, of the nearly 209,000 women diagnosed with breast cancer each year, about 43,000 die.<sup>1</sup> A majority of the women develop bone metastases, tumor-induced bone destruction, hypercalcemia and spinal cord compression during the advanced stages of breast cancer, thus seriously compromising the lifestyle of the affected patients.<sup>2</sup> Currently, there are only limited therapies for bone metastases. Although the two types of drugs - bisphosphonates, and denosumab, an antibody against RANKL - can inhibit bone resorption, their ability to cure bone metastases remains to be established.<sup>3</sup> Thus, development of novel therapies to treat breast cancer bone metastasis is a major unmet need in medicine.

In the recent years oncolytic adenoviruses have shown some potential in the treatment of cancer.<sup>4-12</sup> In an attempt to develop novel therapeutic approaches for bone metastases, our laboratory has developed oncolytic adenoviruses that would kill the cancer cells and simultaneously express a soluble form of TGF $\beta$  ReceptorII-Fc (sTGF $\beta$ RIIFc) that can target TGF $\beta$  induced signaling pathways.<sup>10-12</sup> We chose to target the TGF $\beta$  pathway because high levels of circulating TGF $\beta$  protein is a poor prognostic marker in breast cancer patients.<sup>13, 14</sup> Furthermore, aberrant TGF $\beta$  signaling at the bone metastasis site has been postulated to be a key factor in the progression of breast cancer bone metastases.<sup>14-19</sup> Therefore, there is growing interest in developing inhibitors of TGF $\beta$  signaling for the treatment of various cancer metastases.<sup>20-24</sup> Using a MDA-MB-231 human breast cancer bone metastasis model in immunodeficient mice, we have recently shown that intravenous delivery of oncolytic adenoviruses, Ad.sT $\beta$ RFc and TAd.sT $\beta$ RFc, in tumor bearing mice are effective in inhibiting the established bone metastases.<sup>11, 12</sup> However, before initiating a clinical trial in breast cancer patients, it is important to examine the efficacy of these oncolytic adenoviruses in an immunocompetent animal model because they have the ability to limit adenoviral replication and thus its efficacy. Keeping that in mind, we have now conducted *in vitro* and *in vivo* studies using a mouse mammary 4T1 tumor cell model. We report here that infection of 4T1 cells with recombinant adenoviruses produced transgene expression, and 4T1 cells supported adenoviral replication and were killed by oncolytic adenoviruses. Although 4T1 cells were resistant to TGF $\beta$ -1-induced cytotoxicity, TGF $\beta$  was able to activate signaling. More importantly, intracardiac inoculation of 4T1 cells in BALB/c mice produced bone metastases and osteolytic lesions, and thus is an appropriate pre-clinical model for our purpose. We report here that intravenous injections of Ad.sT $\beta$ RFc and TAd.sT $\beta$ RFc inhibited the progression of skeletal metastases in BALB/c mice. Based on our findings we believe that oncolytic adenoviruses targeting TGF $\beta$  pathways can be developed for treating breast cancer bone metastases.

## Materials and Methods

### Cell culture

4T1 (ATCC, Manassas, VA) mouse mammary tumor cells, 4T1-luc2 (Caliper life sciences, Hopkinton, MA), MV1Lu (ATCC) mink epithelial cells, and HEK 293 (ATCC, Manassas, VA) human embryonic kidney cells were grown in DMEM containing 10% bovine calf serum (Invitrogen, Grand Island, NY).

### Adenoviral vectors

Adenoviral vectors used in these studies are: Ad(E1-).Null, an E1 minus replication-deficient adenovirus containing no foreign gene; Ad(E1-).GFP, a replication-deficient adenovirus expressing EGFP protein; Ad(E1-).sT $\beta$ RFc, a replication-deficient adenovirus expressing sTGF $\beta$ RIIFc gene; Ad.sT $\beta$ RFc, an oncolytic adenovirus expressing sTGF $\beta$ RIIFc gene (constructed using *dI01/07* mutant of Ad5, containing two deletions in E1A region as previously described)<sup>10</sup> and TAd.sT $\beta$ RFc, an oncolytic adenovirus expressing sTGF $\beta$ RIIFc gene with the human TERT promoter driving the adenoviral replication as published.<sup>25</sup> Adenoviral vectors were grown in HEK 293 cells and purified by double CsCl<sub>2</sub> gradient as described.<sup>26</sup> Viral particle (VP) numbers were determined by measuring OD<sub>260</sub> of the SDS-treated adenoviral solutions.

### Adenoviral replication assay

4T1 cells were plated in 24-well dishes ( $2 \times 10^5$  cells/well). The following day, cells were infected with viral vectors ( $5 \times 10^3$  VPs/cell) and the incubations were continued for 3 days. Cells were then subjected to immunohistochemistry for adenoviral hexon staining using an Adenoviral Titer commercial kit (Clontech, Mountain view, CA) as described earlier.<sup>25, 27</sup> Positive hexon expressing brown cells were photographed, and counted under the microscope to quantify viral replication.

### Cytotoxicity assays

To measure TGF $\beta$ -1-induced cytotoxicity, cells were plated in 96-well plates ( $10^3$  cells/well). The following day, cells were infected with various concentrations of TGF $\beta$ -1 (1–10 ng/ml) (Sigma, St. Louis), and the incubations were continued for 7 days. Cells were washed, fixed and stained with sulforhodamine B (SRB) (Sigma, St. Louis), and the A<sub>564</sub> measured as previously described.<sup>26</sup> Untreated control cells were considered to have 100% survival. To examine viral-induced cytotoxicity, the same protocol was used except 4T1 cells were incubated with various doses of adenoviral vectors for 7 days prior to SRB staining.

### GFP expression

4T1 cells were plated in 6-well dishes ( $4 \times 10^5$  cells/well). The following day, cells were infected with Ad(E1-).GFP ( $2.5 \times 10^4$  VPs/cell) and incubated for 48 hrs. Cells were photographed using a florescent microscope (200 $\times$ ).

### sTGFβRIIFc expression

To examine adenoviral vector-mediated sTGFβRIIFc expression, 4T1 cells were plated in 6-well dishes ( $4 \times 10^5$  cells/well). The following day, cells were infected with various viral vectors ( $2.5 \times 10^4$  VPs/cell). After 24 hrs, media was changed to serum free media, and the incubations continued for another 24 hrs. sTGFβRIIFc expression in the media and the cell lysates were examined by Western blot analyses as previously described.<sup>10</sup> sTGFβRIIFc protein amounts in the media were measured by ELISA using antibodies against the human IgG Fc fragment (Jackson ImmunoResearch) as previously described.<sup>11</sup>

### SMAD phosphorylation

4T1 cells were plated in 6-well plates ( $4 \times 10^5$  cells/well). The following day, cells were serum starved for 6 hrs, and then treated with TGFβ-1 (5 ng/ml) in the absence or presence of sTGFβRIIFc (1 μg/ml) for 1 hr. Cells were analyzed for p-SMAD2, p-SMAD3, and for total SMAD2/3 using Western blots as previously described.<sup>28</sup> The blots were visualized by enhanced chemiluminescence substrate (Amersham Biosciences, Piscataway, NJ).

### IL-11 assays

4T1 cells were plated in 6-well plates ( $2 \times 10^5$  cells per well). The following day, cells were serum starved over night, and then exposed to TGFβ-1 (0.1, 1 or 5 ng/ml) for 48 hrs. Media were analyzed for IL-11 levels by ELISA using the previously described method.<sup>28</sup>

### Animal model

All animal experiments were conducted using animal protocols approved by the IACUC committee of the NorthShore University HealthSystem. To establish bone metastases, 4T1-luc2 cells were injected in the left heart ventricle (day 0) of 4 week old BALB/c mice (Charles River laboratories, Wilmington, MA). On day 4, the mice were subjected to BLI in dorsal and ventral positions using Xenogen IVIS Spectrum imaging equipment (Caliper life sciences, Hopkinton, MA). Photon signals were quantified using living image software 3.0 (Caliper life sciences, Hopkinton, MA) as previously described.<sup>12</sup> Mice were divided into various groups, with statistically indistinguishable BLI signals amongst each group. Various viral vectors were administered via tail vein on days 5 and 7 ( $5 \times 10^{10}$  VPs per injection/mouse, each injection in a 0.1 ml volume). The control group of mice was administered the buffer alone.

### Bioluminescence imaging

Mice were imaged in dorsal and ventral positions on days 7, 11 and 14 using the IVIS Spectrum imaging system (Caliper Life Sciences, Hopkinton, MA). Whole-body BLI signals were used to quantify the metastasis as previously described.<sup>12</sup> Signals in the hind limbs were separately quantified to measure the skeletal metastases as described.<sup>12</sup>

### X-ray radiography

On day 14 following tumor cell injections, mice were also subjected to X-ray radiography in prone position using Faxitron (Faxitron X-ray Corporation, Wheeling, IL). Skeletal lesion

sizes were measured in the femur and tibia of both hind limbs using Image J software as described earlier.<sup>11, 12</sup>

### Statistical evaluation

All statistical analyses were performed using GraphPad Prizm 5 (GraphPad software, San Diego, CA). Data are presented as mean  $\pm$  SEM. To analyze BLI signal progression, a two-way repeated-measure ANOVA followed by Bonferroni post-tests was used. For multiple groups, statistical significance was analyzed using one-way ANOVA followed by Bonferroni post-tests.  $p < 0.05$  was considered a statistically significant difference.

## Results

### 4T1 cells can be infected with human adenoviral vectors

Experiments were conducted to examine the infectability of 4T1 cells with replication-deficient and replication competent adenoviral vectors. 4T1 cells were infected with Ad(E1-).GFP, a non-replicating adenovirus for 48 hrs, and the cells were visualized under a fluorescent microscope. The vast majority of cells produced a strong GFP signal (Figure 1a). In another experiment, cells were infected with Ad(E1-).sT $\beta$ RFc, a replication-deficient adenovirus, and two oncolytic adenoviruses- Ad.sT $\beta$ RFc and TAd.sT $\beta$ RFc. Cell lysates and the extracellular media were subjected to Western blot analyses for sTGF $\beta$ RIIFc expression. Infection of 4T1 cells with Ad(E1-).sT $\beta$ RFc, Ad.sT $\beta$ RFc and TAd.sT $\beta$ RFc resulted in sTGF $\beta$ RIIFc protein production which could be detected in the cell lysates as well as the extracellular media (Figure 1b). The amounts of sTGF $\beta$ RIIFc were quantified in the media using ELISA, and were found to be in the range of 6.21–15.48  $\mu$ g/ml of media (Figure 1c). These results indicate that 4T1 cells can be infected with human adenoviruses and that infection with Ad(E1-).sT $\beta$ RFc, Ad.sT $\beta$ RFc or TAd.sT $\beta$ RFc leads to the production of sTGF $\beta$ RIIFc protein, which is secreted into the media.

### Oncolytic adenoviruses replicate and induce cytotoxicity in 4T1 cells

Next, we examined the replication potential of adenoviral vectors in 4T1 cells. Cells were incubated with various adenoviral vectors ( $5 \times 10^3$  VPs/cell) at 37 $^\circ$  for 72 hrs, and viral titer was determined by hexon staining. Figure 2a shows typical hexon staining of 4T1 cells exposed to various viral vectors. There were very few hexon expressing brown cells in Ad(E1-).Null or Ad(E1-).sT $\beta$ RFc treated samples (Figure 2a). However, a large number of 4T1 cells infected with Ad.sT $\beta$ RFc or TAd.sT $\beta$ RFc were hexon positive (Figure 2a). Quantification of hexon positive cells indicated that Ad.sT $\beta$ RFc produced viral titers (Figures 2b, c) which were about 257-times higher than the non-replicating adenovirus Ad(E1-).Null ( $p < 0.001$ ). TAd.sT $\beta$ RFc produced 175-times higher viral titer than Ad(E1-).Null ( $p < 0.01$ ) (Figures 2b, c). However viral titers in Ad(E1-).sT $\beta$ RFc infected cells were similar to those in Ad(E1-).Null treated cells (Figures 2b, c). From these results we conclude that continuous incubation of 4T1 cells with oncolytic adenoviruses can produce viral replication.

To examine if viral replication can result in cytotoxicity, 4T1 cells were incubated with various adenoviral vectors for 7 days, and the cytotoxicity assays were performed. Both the

oncolytic adenoviruses, Ad.sT $\beta$ RFc and TAd.sT $\beta$ RFc produced a dose-dependent cytotoxicity in 4T1 cells (Figure 2d). Based on the IC<sub>50</sub> values, Ad.sT $\beta$ RFc and TAd.sT $\beta$ RFc were about 34.2-fold and 24.0-fold, respectively, more toxic than the non-replicating virus Ad(E1-).Null (Figure 2e). In contrast, a non-replicating virus Ad(E1-).sT $\beta$ RFc produced toxicity that was comparable to Ad(E1-).Null (Figures 2d, e).

#### 4T1 cells are resistant to killing by TGF $\beta$ , but retain TGF $\beta$ -mediated signaling pathways

Next, we investigated the killing effect of TGF $\beta$  in 4T1 cells. 4T1 cells were exposed to various concentrations of TGF $\beta$ -1, and 7 days later cytotoxicity was measured. As a positive control, another rodent cell type MV1Lu, known to be sensitive to TGF $\beta$  was used. As shown in Figure 3a, there was little to no cytotoxic effect of TGF $\beta$ -1 even at the highest concentration used (10 ng/ml) in 4T1 cells. However, MV1Lu cells were killed even by a very low concentration of TGF $\beta$ -1, with an IC<sub>50</sub> of less than 0.1 ng/ml.

To examine if TGF $\beta$  could induce signaling in 4T1 cells, we exposed 4T1 cells to TGF $\beta$ -1 and analyzed the cell lysates for SMAD2 and SMAD3 phosphorylation. Figure 3b shows that TGF $\beta$ -1 induced SMAD2 and SMAD3 phosphorylation in 4T1 cells. Co-incubation of sTGF $\beta$ RIIFc with TGF $\beta$ -1 inhibited TGF $\beta$ -1-dependent SMAD2 and SMAD3 phosphorylation (Figure 3b). We also examined the effect of TGF $\beta$ -1 on IL-11 production, a known osteolytic factor in human breast cancer cells.<sup>28, 29</sup> TGF $\beta$ -1 induced IL-11 protein production in a dose dependent manner (Figure 3c). These results indicate that 4T1 cells respond to TGF $\beta$ -1 and undergo activation of signaling pathways that are known to favor bone metastases in human breast cancer cells.<sup>18, 28, 30</sup> Importantly, sTGF $\beta$ RIIFc is able to abolish the TGF $\beta$  signaling.

#### Oncolytic adenoviral-mediated inhibition of 4T1-induced metastases: BLI analyses

Next, we examined the effect of systemic administration of adenoviral vectors expressing sTGFRIIFc in a 4T1 bone metastasis model. 4T1-luc2 cells were inoculated into the left heart ventricles of BALB/c mice. After four days, mice were subjected to whole-body BLI in both dorsal and ventral positions. Mice were split into multiple groups, with nearly equal BLI signal within each group. Mice were split into multiple groups, with nearly equal BLI signal within each group. Two doses of adenoviral vectors were given via the tail vein- the first dose on day 5 ( $5 \times 10^{10}$  VPs/mouse) and a second dose on day 7 ( $5 \times 10^{10}$  VPs/mouse). Mice were subjected to BLI on days 7, 11 and 14 following tumor cell injection. A representative mouse showing BLI signal from each treatment group is shown in Figure 4a. Whole-body BLI signals were quantified and are shown in Figure 4b. There was a time-dependent increase in the whole-body BLI signal to  $0.88 \times 10^{11}$  photons/sec in the control group of mice that received buffer alone (Figure 4b). There was no significant inhibition of BLI signal in the Ad(E1-).Null, Ad(E1-).sT $\beta$ RFc or TAd.sT $\beta$ RFc treatment groups (Figure 4b). However, Ad.sT $\beta$ RFc induced a significant inhibition ( $p < 0.05$ ) of the whole-body BLI. Since 4T1 cells also established bone metastasis in the hind limbs (Figure 4a), the effect of viral vectors on the BLI signal in the hind limbs was quantified. In the control group of mice, the BLI signal in the hind limbs reached to  $0.86 \times 10^{10}$  photons/sec, and there was a significant inhibition of BLI signal accumulation in the hind limbs in the Ad.sT $\beta$ RFc treated

group ( $p < 0.05$ ). However, Ad(E1-).Null, Ad(E1-).sT $\beta$ RFc and TAd.sT $\beta$ RFc treatments had no significant effect on the BLI signal intensity in the hind limbs (Figure 4c).

### Oncolytic adenoviral vectors'-mediated inhibition of 4T1-induced metastases: X-ray analyses

To further examine the effects of vectors' administration on bone metastases, mice were subjected to X-ray radiography on day 14. A representative example of X-ray radiographs from each group is shown in Figure 5a. The long bones in buffer-treated and Ad(E1-).Null-treated mice had large osteolytic lesions, as indicated by red arrows. The lesion sizes were relatively smaller in the other treatment groups. The tumor lesions in the hind limbs were quantified using the Image J program and are shown in Figure 5b. Tumor sizes in the buffer group were  $6.92 \pm 1.27 \text{ mm}^2$ . Tumor sizes in Ad(E1-).Null, Ad(E1-).sT $\beta$ RFc, and Ad.sT $\beta$ RFc and TAd.sT $\beta$ RFc treatment groups were  $5.79 \pm 0.86$ ,  $3.56 \pm 0.72$ ,  $2.30 \pm 0.69$ , and  $2.94 \pm 0.57 \text{ mm}^2$ , respectively. These results indicate that while Ad(E1-).Null and Ad(E1-).sT $\beta$ RFc had no significant effect on the tumor sizes, a significant inhibition of the tumor growth was observed in the Ad.sT $\beta$ RFc ( $p < 0.01$ ) and TAd.sT $\beta$ RFc ( $p < 0.05$ ) treatment groups (Figure 5b).

While we were able to monitor BLI and X-ray until day 14, by day 18 a number of animal deaths were observed in each of the treatment groups. The following ratios indicate the number of mice that died between days 14 and 18 over the initial number of mice in each group: buffer: 3/9; Ad(E1-).Null: 4/9; Ad(E1-).sT $\beta$ RFc: (3/9); Ad.sT $\beta$ RFc: 2/11; and TAd.sT $\beta$ RFc: 3/11. To confirm Ad(E1-).sT $\beta$ RFc, Ad.sT $\beta$ RFc and TAd.sT $\beta$ RFc-mediated sTGF $\beta$ RIIFc expression in the blood, samples were collected from the remaining mice on day 18 and the sTGF $\beta$ RIIFc production was analyzed by ELISA. The results indicated high levels:  $2.43 \pm 1.67 \text{ }\mu\text{g/ml}$ ,  $6.53 \pm 16.31 \text{ }\mu\text{g/ml}$ ,  $15.41 \pm 24.86 \text{ }\mu\text{g/ml}$  of sTGF $\beta$ RIIFc in blood samples from Ad(E1-).sT $\beta$ RFc, Ad.sT $\beta$ RFc and TAd.sT $\beta$ RFc treatment groups, respectively. Thus, while the intravenous injection of Ad(E1-).sT $\beta$ RFc, Ad.sT $\beta$ RFc and TAd.sT $\beta$ RFc resulted in sTGF $\beta$ RIIFc production, it appears that the replicating viruses expressing sTGF $\beta$ RIIFc were the most effective in inhibiting bone metastases.

## Discussion

The key finding here is that intravenous delivery of oncolytic virus Ad.sT $\beta$ RFc expressing sTGF $\beta$ RIIFc can inhibit bone metastasis in the 4T1 mouse mammary tumor bone metastasis model in a syngeneic host as revealed by BLI studies. X-ray radiographic analyses showed inhibition of tumor growth by Ad.sT $\beta$ RFc and TAd.sT $\beta$ RFc, though Ad.sT $\beta$ RFc was superior to TAd.sT $\beta$ RFc. A non-replicating virus, Ad(E1-).sT $\beta$ RFc, expressing sTGF $\beta$ RIIFc showed some inhibition of bone metastasis in X-ray analyses; Ad(E1-).Null was not effective in either BLI or X-ray analyses.

Most of the previously published studies using oncolytic adenoviruses have been conducted in human xenografts established in immunodeficient nude mice, mainly because mouse tumor cells are not considered good targets for the human adenoviruses. However, it is critical that we continue to explore the animal models in which oncolytic adenoviruses can be examined in immunocompetent syngeneic hosts as described here. It is quite interesting

that 4T1 cells can be infected with human adenoviruses resulting in high levels of transgene expression indicating the presence of adenoviral receptors even in mouse 4T1 cells. Moreover, continuous exposure of 4T1 cells to oncolytic adenoviral vectors can produce a viral titer. This indicates that human adenoviruses can result in virus entry and replication, clearly demonstrating that human adenoviruses can indeed infect and replicate in 4T1 mouse tumor cells, which is consistent with a previous report<sup>31</sup> This infection could be via the previously known adenoviral receptor, by an unknown adenoviral receptor or even by other pathways including clathrin independent mechanisms such as macropinocytosis, phagocytosis, or trans-endocytosis.<sup>32</sup> Once the viral particles are internalized by the cells, however, viral replication proceeds as in human breast cancer cells. While the exact relationship of the Ad.sT $\beta$ RFc and TAd.sT $\beta$ RFc-induced replication resulting in the cytotoxicity of the 4T1 tumor model remains to be examined, it is tempting to speculate that the viral replication resulting in the cytotoxic effects of the adenoviral vectors in the mouse tumor cells could play a role in mediating the *in vivo* anti-tumor responses reported here.

Another important observation is the inability of TGF $\beta$  to kill 4T1 cells and yet induce the TGF $\beta$  signaling pathway (SMAD-phosphorylation), and the production of IL-11 (a well known osteolytic factor in human breast cancer bone metastasis). Thus, in this regard 4T1 is an appropriate tumor model for examining the role of TGF $\beta$  signaling in bone metastases. In the radiographic analyses, a non-replicating adenovirus expressing sTGF $\beta$ RIIFc showed some inhibition of bone metastasis, albeit weaker than oncolytic adenovirus Ad.sT $\beta$ RFc. Again, these studies suggest that the expression of sTGF $\beta$ RIIFc, coupled with viral replication and cytotoxicity, is potentially playing a role in mediating the inhibition of bone metastases.

Intravenous delivery of adenoviruses will result in their uptake mainly in the liver, and in smaller amounts in other tissues and the skeletal tumors.<sup>11, 12, 27, 33</sup> We believe that the infection of tumor cells *in vivo* will result in the viral replication in the tumor cells causing cell killing and partial tumor destruction. Infection of tumor cells and other mouse organs will result in the production of sTGF $\beta$ RIIFc that will be released in the blood. The sTGF $\beta$ RIIFc production resulting in the inhibition of TGFs signaling at the tumor/bone site will also contribute towards the inhibition of bone metastases. Among the three vectors expressing sTGF $\beta$ RIIFc, the most effective vector is Ad.sTsRFc; TAd.sTsRFc is slightly weaker than Ad.sTsRFc, and the least effective is Ad(E1-).sTsRFc. Since all three vectors produce nearly equal amounts of sTGF $\beta$ RIIFc, Ad.sTsRFc is the most effective, which is perhaps due to its higher replication potential in the tumor cells. TAd.sTsRFc can also replicate in the tumor cells, but its replication potential is slightly lower than Ad.sTsRFc; and Ad(E1-).sTsRFc is replication-deficient. Based on these results, we believe that both viral replication and the sTGF $\beta$ RIIFc expression play an important role in the inhibition of bone metastases.

In addition to understanding the role of viral replication and the inhibition of TGF $\beta$  signaling at the tumor-bone microenvironment, the future availability of a 4T1 bone metastasis model will also allow us to further explore the role of the adenoviral vector-induced innate and humoral immune responses<sup>34-36</sup>, the role of TGF $\beta$  in suppressing the immune system<sup>14, 15, 37</sup> and how that can be reversed by the oncolytic adenoviruses expressing



sTGF $\beta$ RIIFc. These questions can be addressed only in fully immune competent animal models.

In conclusion, our work described here shows that oncolytic adenoviruses targeting the TGF $\beta$  pathway can inhibit breast cancer bone metastases in a mouse mammary tumor model established in a syngeneic immunocompetent host and represents an important step in developing oncolytic adenoviruses for the treatment of breast cancer bone metastases. This animal model will now allow us to investigate the underlying molecular mechanism of action of the oncolytic adenoviruses, which may help in refining this method of treatment.

## Acknowledgments

The research described here was funded by a grant from the National Cancer Institutes grant # R01CA127380 (P.S.). We are thankful to Janardan Khandekar, Theodore Mazzone, Bruce Brockstein and an anonymous source for their generous support.

## References

1. Cancer Facts and Figures. American Cancer Society; 2011. <http://www.cancer.org/Research/cancer-facts-figures-2011>
2. Coleman RE. Metastatic bone disease: clinical features, pathophysiology and treatment strategies. *Cancer Treat Rev.* 2001; 27(3):165–76. [PubMed: 11417967]
3. Candelaria-Quintana D, Dayao ZR, Royce ME. The role of antiresorptive therapies in improving patient care in early and metastatic breast cancer. *Breast Cancer Res Treat.* 2012; 132:355–363. [PubMed: 21987034]
4. Crompton AM, Kirn DH. From ONYX-015 to armed vaccinia viruses: the education and evolution of oncolytic virus development. *Curr Cancer Drug Targets.* 2007; 7(2):133–9. [PubMed: 17346104]
5. Toth K, Dhar D, Wold WS. Oncolytic (replication-competent) adenoviruses as anticancer agents. *Expert Opin Biol Ther.* 2010; 10(3):353–68. [PubMed: 20132057]
6. Bischoff JR, Kirn DH, Williams A, Heise C, Horn S, Muna M, et al. An adenovirus mutant that replicates selectively in p53-deficient human tumor cells. *Science.* 1996; 274(5286):373–6. [PubMed: 8832876]
7. Reid T, Warren R, Kirn D. Intravascular adenoviral agents in cancer patients: lessons from clinical trials. *Cancer Gene Ther.* 2002; 9(12):979–86. [PubMed: 12522437]
8. Nemunaitis J, Cunningham C, Buchanan A, Blackburn A, Edelman G, Maples P, et al. Intravenous infusion of a replication-selective adenovirus (ONYX-015) in cancer patients: safety, feasibility and biological activity. *Gene Ther.* 2001; 8(10):746–59. [PubMed: 11420638]
9. Nemunaitis J, Tong AW, Nemunaitis M, Senzer N, Phadke AP, Bedell C, et al. A phase I study of telomerase-specific replication competent oncolytic adenovirus (telomelysin) for various solid tumors. *Mol Ther.* 2010; 18(2):429–34. [PubMed: 19935775]
10. Seth P, Wang ZG, Pister A, Zafar MB, Kim S, Guise T, et al. Development of oncolytic adenovirus armed with a fusion of soluble transforming growth factor-beta receptor II and human immunoglobulin Fc for breast cancer therapy. *Hum Gene Ther.* 2006; 17(11):1152–60. [PubMed: 17032151]
11. Hu Z, Zhang Z, Guise T, Seth P. Systemic Delivery of an Oncolytic Adenovirus Expressing Soluble Transforming Growth Factor-beta Receptor II-Fc Fusion Protein Can Inhibit Breast Cancer Bone Metastasis in a Mouse Model. *Hum Gene Ther.* 2010; 21(11):1623–1629. [PubMed: 20712434]
12. Hu Z, Gerseny H, Zhang Z, Chen YJ, Berg A, Stock S, et al. Oncolytic Adenovirus Expressing Soluble TGFbeta Receptor II-Fc-mediated Inhibition of Established Bone Metastases: A Safe and Effective Systemic Therapeutic Approach for Breast Cancer. *Mol Ther.* 2011; 9:1609–1618. [PubMed: 21712815]

13. Teicher BA. Malignant cells, directors of the malignant process: role of transforming growth factor-beta. *Cancer Metastasis Rev.* 2001; 20(1-2):133-43. [PubMed: 11831642]
14. Barcellos-Hoff MH, Akhurst RJ. Transforming growth factor-beta in breast cancer: too much, too late. *Breast Cancer Res.* 2009; 11(1):202. [PubMed: 19291273]
15. Padua D, Massague J. Roles of TGFbeta in metastasis. *Cell Res.* 2009; 19(1):89-102. [PubMed: 19050696]
16. Buijs JT, Stayrook KR, Guise TA. TGF-beta in the Bone Microenvironment: Role in Breast Cancer Metastases. *Cancer Microenviron.* 2011; 4:261-281. [PubMed: 21748439]
17. Guise TA, Mohammad KS, Clines G, Stebbins EG, Wong DH, Higgins LS, et al. Basic mechanisms responsible for osteolytic and osteoblastic bone metastases. *Clin Cancer Res.* 2006; 12(20 Pt 2):6213s-6216s. [PubMed: 17062703]
18. Kang Y, He W, Tulley S, Gupta GP, Serganova I, Chen CR, et al. Breast cancer bone metastasis mediated by the Smad tumor suppressor pathway. *Proc Natl Acad Sci U S A.* 2005; 102(39):13909-14. [PubMed: 16172383]
19. Akhtari M, Mansuri J, Newman KA, Guise TM, Seth P. Biology of breast cancer bone metastasis. *Cancer Biol Ther.* 2007; 7(1):3-9. [PubMed: 18059174]
20. Muraoka RS, Dumont N, Ritter CA, Dugger TC, Brantley DM, Chen J, et al. Blockade of TGF-beta inhibits mammary tumor cell viability, migration, and metastases. *J Clin Invest.* 2002; 109(12):1551-9. [PubMed: 12070302]
21. Yang YA, Dukhanina O, Tang B, Mamura M, Letterio JJ, MacGregor J, et al. Lifetime exposure to a soluble TGF-beta antagonist protects mice against metastasis without adverse side effects. *J Clin Invest.* 2002; 109(12):1607-15. [PubMed: 12070308]
22. Iyer I, Wang Z-G, Akhtari M, Zhao W, Seth P. Targeting TGF beta signaling for cancer therapy. *Cancer Biol Ther.* 2005; 4(3):261-6. [PubMed: 15846079]
23. Nagaraj NS, Datta PK. Targeting the transforming growth factor-beta signaling pathway in human cancer. *Expert Opin Investig Drugs.* 2010; 19(1):77-91.
24. Juarez P, Guise TA. TGF-beta in cancer and bone: implications for treatment of bone metastases. *Bone.* 2011; 48(1):23-9. [PubMed: 20699127]
25. Hu Z, Robbins JS, Pister A, Zafar MB, Zhang ZW, Gupta J, et al. A modified hTERT promoter-directed oncolytic adenovirus replication with concurrent inhibition of TGFbeta signaling for breast cancer therapy. *Cancer Gene Ther.* 2010; 17(4):235-43. [PubMed: 19798122]
26. Katayose D, Gudas J, Nguyen H, Srivastava S, Cowan KH, Seth P. Cytotoxic effects of adenovirus-mediated wild-type p53 protein expression in normal and tumor mammary epithelial cells. *Clin Cancer Res.* 1995; 1(8):889-97. [PubMed: 9816059]
27. Zhang Z, Krimmel J, Hu Z, Seth P. Systemic Delivery of a Novel Liver-Detargeted Oncolytic Adenovirus Causes Reduced Liver Toxicity but Maintains the Antitumor Response in a Breast Cancer Bone Metastasis Model. *Hum Gene Ther.* 2011; 22:1137-1142. [PubMed: 21480822]
28. Gupta J, Robbins J, Jilling T, Seth P. TGFbeta-dependent induction of Interleukin-11 and Interleukin-8 involves SMAD and p38 MAPK pathways in breast tumor models with varied bone metastases potential. *Cancer Biol Ther.* 2011; 11(3):311-116. [PubMed: 21099351]
29. Nguyen DX, Massague J. Genetic determinants of cancer metastasis. *Nat Rev Genet.* 2007; 8(5):341-52. [PubMed: 17440531]
30. Korpala M, Yan J, Lu X, Xu S, Lerit DA, Kang Y. Imaging transforming growth factor-beta signaling dynamics and therapeutic response in breast cancer bone metastasis. *Nat Med.* 2009; 15(8):960-6. [PubMed: 19597504]
31. Guo W, Zhu H, Zhang L, Davis J, Teraishi F, Roth JA, et al. Combination effect of oncolytic adenovirotherapy and TRAIL gene therapy in syngeneic murine breast cancer models. *Cancer Gene Ther.* 2006; 13(1):82-90. [PubMed: 16037823]
32. Doherty GJ, McMahon HT. Mechanisms of endocytosis. *Annu Rev Biochem.* 2009; 78:857-902. [PubMed: 19317650]
33. Waddington SN, McVey JH, Bhella D, Parker AL, Barker K, Atoda H, et al. Adenovirus serotype 5 hexon mediates liver gene transfer. *Cell.* 2008; 132(3):397-409. [PubMed: 18267072]

34. Thomas MA, Spencer JF, Toth K, Sagartz JE, Phillips NJ, Wold WS. Immunosuppression enhances oncolytic adenovirus replication and antitumor efficacy in the Syrian hamster model. *Mol Ther.* 2008; 16(10):1665–73. [PubMed: 18665155]
35. Bessis N, GarciaCozar FJ, Boissier MC. Immune responses to gene therapy vectors: influence on vector function and effector mechanisms. *Gene Ther.* 2004; 11 (Suppl 1):S10–17. [PubMed: 15454952]
36. Ahi YS, Bangari DS, Mittal SK. Adenoviral vector immunity: its implications and circumvention strategies. *Curr Gene Ther.* 2011; 11(4):307–20. [PubMed: 21453277]
37. Nam JS, Terabe M, Kang MJ, Chae H, Voong N, Yang YA, et al. Transforming growth factor beta subverts the immune system into directly promoting tumor growth through interleukin-17. *Cancer Res.* 2008; 68(10):3915–23. [PubMed: 18483277]

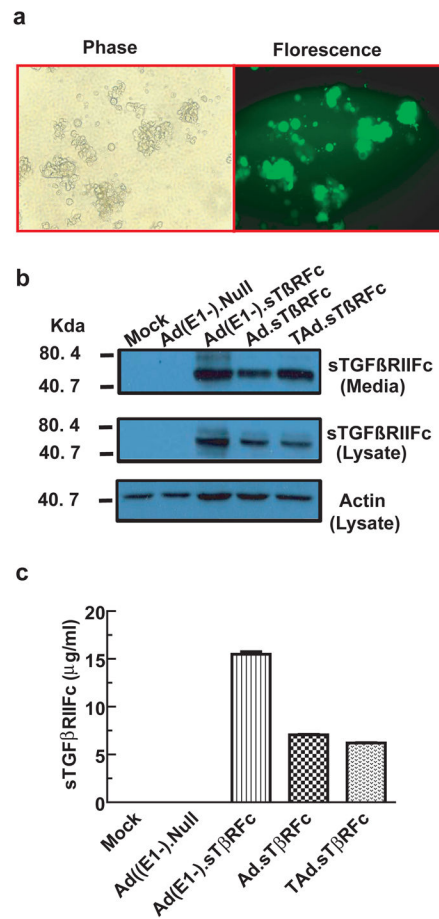


**Figure 1.**

Adenoviral-mediated transgene expression in 4T1 cells. **(a)** 4T1 cells were infected with Ad(E1-).GFP ( $2.5 \times 10^4$  VPs/cell) for 24 hrs. Cells were photographed ( $200\times$ ) using a fluorescent microscope. Same viewing fields were used to take phase contrast (left) or fluorescent (right) images. **(b)** 4T1 cells were infected with various adenoviral vectors ( $2.5 \times 10^4$  VPs/cell). Cell lysates and media were analyzed by Western blots for sTGFβRIIFc protein expression. **(c)** Extracellular media were used to examine sTGFβRIIFc levels by ELISA method.

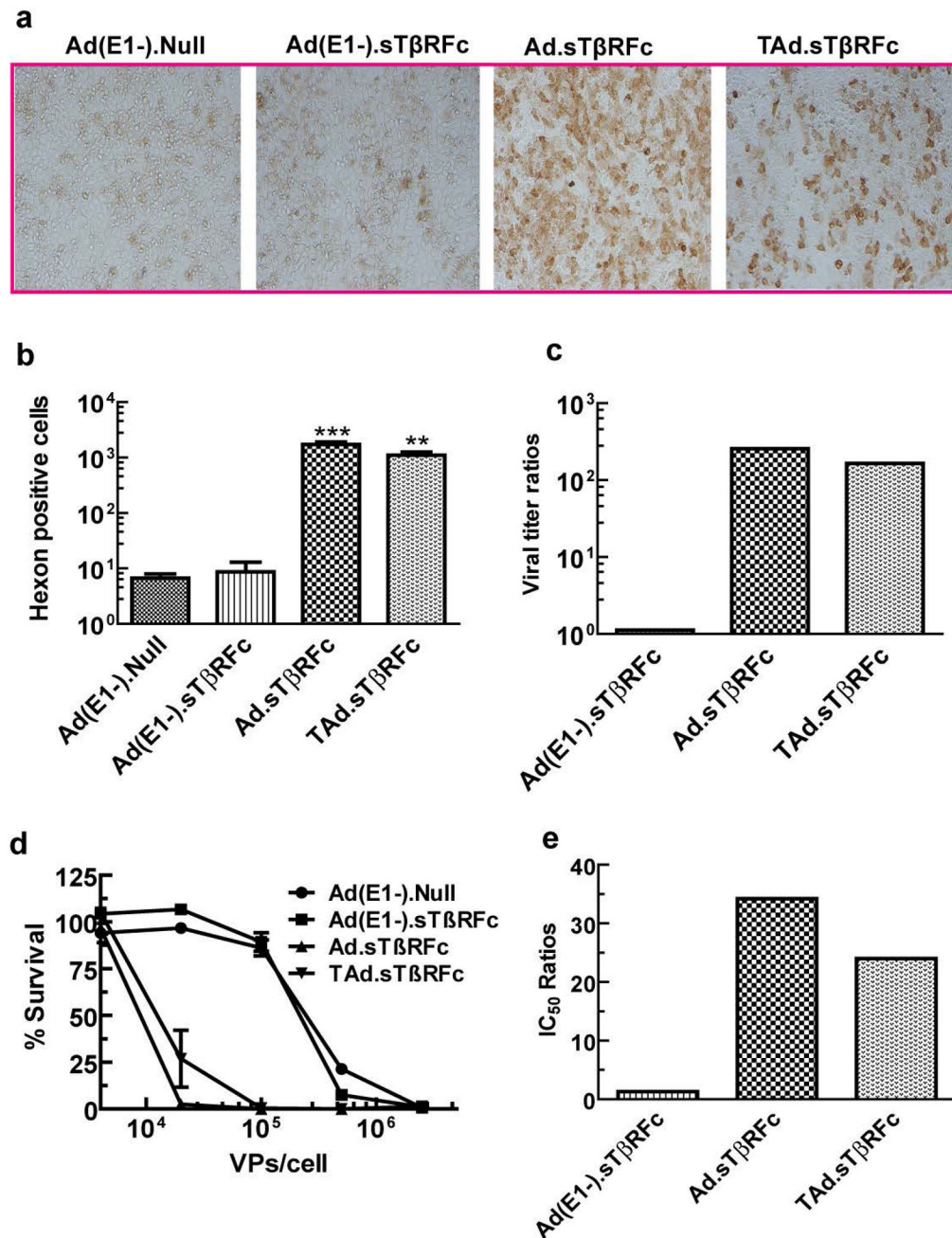


**Figure 2.**

Adenoviral replication and cytotoxicity in 4T1 cells. (a) 4T1 cells were infected with various viral vectors for 72 hrs, and stained for hexon protein. (b) Hexon positive cells were counted in each well to measure the viral titers. (c) The ratios between the viral titer of each virus and that of Ad(E1-).Null are shown. (d) 4T1 cells were exposed to various viral vectors for 7 days. The cytotoxicity assays were conducted by SRB staining. Control cells were considered to have 100% survival. (e) IC<sub>50</sub> for each virus was calculated, and the IC<sub>50</sub> ratios between each vector and Ad(E1-).Null are shown. \*\*\* represents p<0.001, \*\* represents p<0.01.

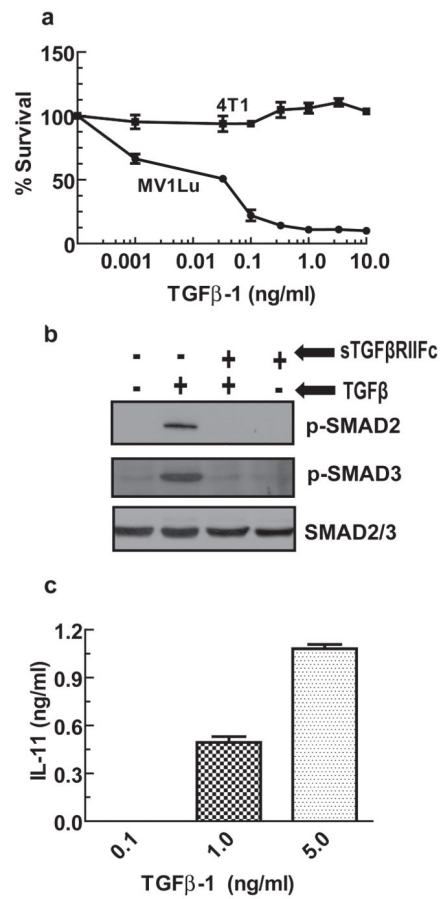


**Figure 3.**

Effect of TGFβ-1 on 4T1 cells. **(a)** 4T1 or MV1Lu cells were exposed to various concentrations of TGFβ-1. After 7 days, cytotoxicity assays were conducted using SRB staining. Control cells were considered to have 100% survival. **(b)** 4T1 cells were exposed to TGFβ-1 (1 ng/ml) for 60 minutes in the absence or presence of sTGFβRIIFc (250 ng/ml). Cell lysates were examined for p-SMAD2, p-SMAD3 and total SMAD2/3 by Western blot analysis. **(c)** 4T1 cells were exposed to various concentrations of TGFβ-1 for 48 hrs. Cell media were used to measure IL-11 levels by ELISA method.

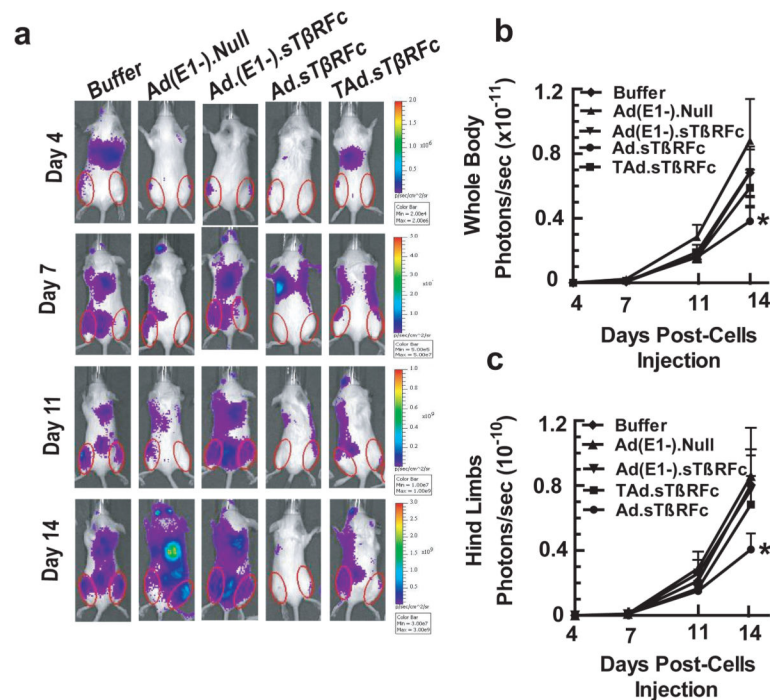


**Figure 4.**

Effect of systemic delivery of viral vectors on 4T1 bone metastases: BLI analysis. 4T1-luc2 cells were injected in BALB/c mice ( $5 \times 10^4$  cells/mouse) on day 0. Initial BLI was performed on day 4; mice with positive tumors were administered viral vectors or buffer (via tail vein) on day 5 and day 7. **(a)** BLI was conducted on days 7, 11 and 14. The numbers of mice in each treatment group were: buffer (n=9), Ad(E1-).Null (n=9), Ad(E1-).sTβRFc (n=9), Ad.sTβRFc (n=11) and TAd.sTβRFc (n=11). Representative mice of each treatment group are shown. **(b)** BLI signal in the whole body of mice in various treatment groups were quantified and are shown. **(c)** To measure bone metastases, BLI signals in the hind limbs (shown by red circles) were quantified in each treatment group and are shown. \* represents  $p < 0.05$ .

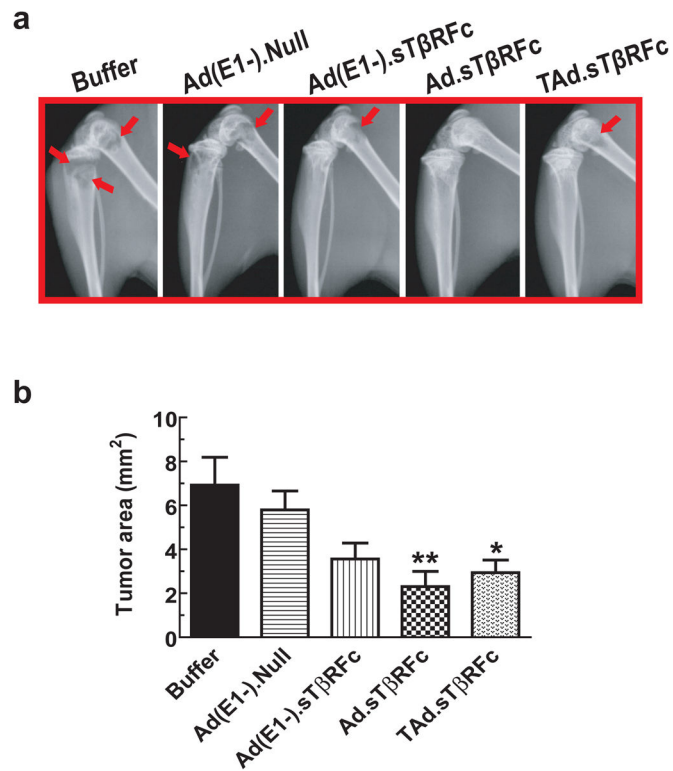


**Figure 5.**

Effect of systemic delivery of viral vectors on 4T1 bone metastases: X-ray radiography. **(a)** Mice from the above experiment described in Figure 4, were subjected to X-ray radiography on day 14. **(b)** Lesion sizes in each mouse were calculated using Image J software. Results shown are the average lesion sizes in the hind limbs in each of the treatment groups. The numbers of mice in each treatment group were: buffer (n=9), Ad(E1-).Null (n=9), Ad(E1-).sTβRFc (n=9), Ad.sTβRFc (n=11) and TAd.sTβRFc (n=11). \* represents  $p < 0.05$ , \*\* represents  $p < 0.01$ .